THE ROLE OF NITRIC OXIDE IN THE ADAPTATION OF CEREBROCORTICAL MICROCIRCULATION TO UNILATERAL COMMON CAROTID ARTERY OCCLUSION

PhD thesis

László Hricisák

Doctoral School of Theoretical and Translational Medicine

Semmelweis University

Supervisor: Zoltán Benyó, MD, DSc

Official reviewers: Rita Benkő, PhD

Attila Jósvai, MD, PhD

Head of the Final Examination Committee:

Tamás Radovits, MD, PhD

Members of the Final Examination Committee:

Rudolf Urbanics, MD, PhD

Dániel Veres, MD, PhD

Budapest

2024

1. Introduction

The autoregulation of cerebral circulation is of utmost importance to maintain and reestablish the optimal oxygen and nutrient supply of neurons in the case of disturbances in the cardiovascular system. Impaired autoregulational capacity and sudden changes in cerebrocortical blood flow (CoBF) can lead not only to severe cerebrovascular diseases but indirectly also to several social and economic consequences.

One of the key factors determining the effectiveness of cerebral microcirculatory blood flow autoregulation is vasodilator molecules, of which nitric oxide (NO) is thought to have utmost importance. NO, first identified as a potent vasodilator and a regulator of blood flow and pressure, also plays a crucial role in regulating vascular smooth muscle tone, leukocyte activation, platelet aggregation, interactions between the endothelium and circulating cells, and vascular smooth muscle cell proliferation. NO is produced by three isoforms of nitric oxide synthases (NOS): neuronal NOS (NOS1 or nNOS), endothelial NOS (NOS3 or eNOS), and inducible NOS (NOS2 or iNOS). NOS1 can be found in the peripheral non-adrenergic and non-cholinergic (NANC) autonomic nervous system, acting as an atypical neurotransmitter relaxing vascular and non-vascular smooth muscle. The inducible NOS isoform (NOS2) has a significant role during sepsis and inflammation. NO produced by NOS3 in the endothelial cells is a physiologically important vasodilator. Various factors can increase the activation of NOS3, such as the increase in intracellular Ca^{2+} concentration or the phosphorylation of the enzyme.

2. Objectives

Our aim was to investigate the role of NO in cerebrovascular adaptation in a model of unilateral carotid artery flow cessation. Four preclinical mouse models of impaired NO synthesis were utilized: in the first set of studies, we aimed to test the role of NOS3 in cerebrovascular compensatory mechanisms after unilateral occlusion of the common carotid artery (CCA). Subsequently, NOS1 knockout (NOS1 KO) mice, NOS1 and NOS3 double knockout (NOS1/3 DKO) mice, and control mice treated with L-NAME, an inhibitor of NO synthesis, were also investigated. The effects of unilateral carotid artery occlusion (CAO) on ipsi- and contralateral regional, hemispheric blood flow were assessed using laser-speckle contrast imaging (LSCI). In the second set of studies, morphological differences in pial anastomoses, which represent an alternative way for the blood flow to the ischemic regions, were also examined. Based on previous evidence, we hypothesized that impaired availability of vasodilator NO compromises CBF homeostasis by altering inter- and intrahemispheric blood flow redistribution after unilateral disruption of carotid artery flow. We also hypothesized that the existence of compensatory pathways activated in genetically modified animals may result in a less severe impairment of adaptation. Therefore, L-NAME treatment was used to identify the effects of acute NO deficiency in vivo.

3. Materials and Methods

3.1 Experimental animals

Male mice with a C57Bl6/N genetic background, aged between 12 and 17 weeks, served as control animals in this study. To investigate the role of nitric oxide synthases (NOSs) after unilateral CAO,

three genetically modified mouse models were employed: NOS3 knockout (NOS3 KO), NOS1 knockout (NOS1 KO) and NOS1/3 double knockout (NOS1/3 DKO). Additionally, a pharmacological approach was also employed, using L-NAME treatment in control animals to inhibit NO synthesis by all NOS isoforms. The animals were housed in a specific pathogen-free animal facility with a 12/12 hours dark/light cycle, and they had access to food and water ad libitum. All experimental procedures were conducted in accordance with the guidelines of the Hungarian Law of Animal Protection (XXVIII/1998) and adhered to the ARRIVE (Animal Research: Reporting In Vivo Experiments) guidelines. Ethical approval for the study was obtained from the National Scientific Ethical Committee on Animal Experimentation (ÁTET, PEI/001/2706-13/2014, approval date: 17 December 2014; PE/EA/487-6/2021, approval date: 9 November 2021).

3.2 Surgical procedures

The animals were positioned on a heating pad beneath a stereotaxic microscope under 2% isoflurane anesthesia. A rectal probe connected to the controlled heating pad was employed to ensure stable body temperature throughout the experiment. The depth of anesthesia was regularly assessed by monitoring plantar and corneal reflexes. The level of anesthesia was deepened whenever any signs of pain or arousal were observed. After that, a small incision was made on the left hindlimb, and a PE 50 cannula was inserted into the femoral artery. The cannulation served to measure systemic arterial blood pressure during the experiment and allowed blood sample collection at the end of the procedure. Subsequently, the anesthesia was switched to intraperitoneal ketamine (100 μg/g body weight) and xylazine (10 μg/g

body weight). This anesthesia regimen was maintained for the remaining part of the experiment. A PE 10 tracheal cannula was introduced to facilitate spontaneous respiration. Thereafter, the left carotid sheath was dissected precisely, avoiding contact or damage to the vagus nerve. Once the common carotid artery was exposed, a loop was gently positioned around it for later occlusion during the experimental procedures.

3.3 Measurement of CAO-induced changes in cerebrocortical blood flow (CoBF)

After completing the aforementioned surgical procedures, the animals were placed in a stereotaxic head holder on a heating pad under the laser speckle instrument. Care was taken to secure the heads of the animals to prevent any movements that could introduce artifacts in the recordings. The femoral artery cannula was connected to a pressure sensor to enable the measurement of systemic arterial blood pressure. For the assessment of changes in CoBF, the LSCI method was employed. The LSCI instrument used was precisely positioned 10 cm above the previously exposed skull, which was accomplished by retracting the skin following a small midline incision. Thereafter, atipamezole (1 µg/g i.p.) was administered as an antidote to counteract the blood pressure-lowering effects of xylazine. After stabilization of the blood pressure, L-NAME (10 mg/kg i.p.) was administered intraperitoneally to a group of control animals, and a 30-minute waiting period was ensured. Subsequently, baseline measurements of CoBF and blood pressure were obtained, taking approximately 10 minutes. Following these baseline measurements, the unilateral common carotid artery occlusion (CAO) procedure was performed by tightening the previously loose knot around the vessel. After five

minutes of recording, an arterial blood sample was collected through the femoral cannula into a heparin-coated capillary for subsequent blood gas analysis. The Radiometer ABL80Flex instrument was used to assess the blood gas and acid-base parameters. Experiments only with arterial blood gas parameters falling within the physiological range (pO_2>90 mmHg, pCO_2 between 25 and 55 mmHg) were included in the analysis.

The original CoBF data, initially measured in arbitrary units (AU), were subsequently converted into the percentage of the average baseline value recorded over one minute. These percentage values were then averaged at 15-second intervals, including time points -45s, -30s, -15s, and 0s, the latter representing the time of occlusion after the baseline phase. The percentage values were averaged at 3-second intervals during the first minute following the occlusion. Throughout the rest of the experiment, the percentage values were averaged every 15 seconds. In the first set of experiments, we differentiated the frontal, parietal, and temporal regions. Another region can also be identified between these regions, namely the zone of pial anastomoses. In the second set of experiments, the frontal and the parietal regions were considered as one region, called frontoparietal because, in the first set of studies, no differences had been found between the CoBF changes of these two regions after CAO. To quantify the CoBF changes, the area over the CoBF curve values (AOC, sec*%) were also determined in the acute and subacute phases for each animal in the different cerebrocortical regions.

3.4 Morphological analysis of the cerebrocortical vasculature

In the second set of experiments, cerebrocortical vasculature was visualized by transcardial perfusion of saline solution and black inks. First, in 2% isoflurane anesthesia, 10 mL of heparinized saline solution (10 IU/mL) was injected into the left cardiac ventricle. Subsequently, a 2 mL mixture of drawing ink, endorsing ink, and distilled water in a 6:1:6 ratio was administered to the animals. Then the brains were removed and placed in a 4% formaldehyde solution for fixation. After a minimum of 24 hours, pictures of the dorsal surface of the brains were captured using a digital camera and a Leica microscope. The morphological analysis focused on the collaterals connecting branches of the anterior cerebral artery (ACA) and the middle cerebral artery (MCA). ImageJ software was employed to analyze the acquired pictures. A blinded investigator utilized a micrometer etalon for calibration and performed calculations on the number and tortuosity index of the collaterals in both hemispheres. The tortuosity index was determined by dividing the vessel's curved length by the linear distance between the two ends of the vessel.

3.5 Statistical analyses

The Shapiro-Wilk test was employed to assess the normal distribution of the data. The results are presented as the arithmetic mean, accompanied by the standard error of mean (SEM) when data are normally distributed, and as the median, accompanied by the interquartile range when data are not normally distributed. The significance levels were determined using Student's unpaired t-test (*$p<0.05$, **$p<0.01$, ***$p<0.001$, and ****$p<0.0001$). For experiments involving multiple variables, one-way or two-way repeated measures ANOVA, or Kruskal-Wallis test was utilized, followed by Bonferroni's or Tukey's post

hoc test, depending on the specific number of variables and the normality distribution of the data. Graphs and statistical analyses were performed using GraphPad Prism software.

4. Results

4.1 The role of NOS3

4.1.1 Blood pressure changes in NOS3 KO animals

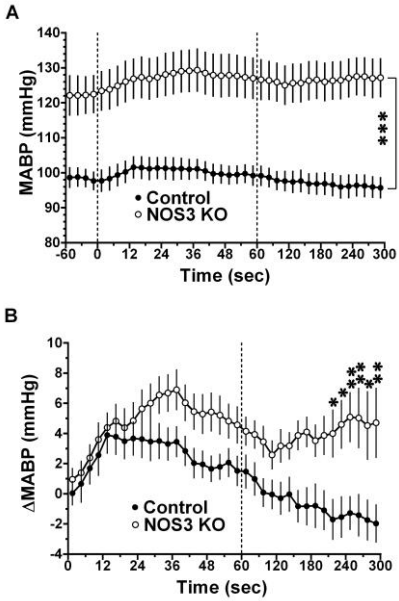

Fig. 1. Mean arterial blood pressure (MABP) in control (n=12) and endothelial nitric oxide synthase knockout (NOS3 KO; n=11) mice (A) and its changes after left carotid artery occlusion (CAO) (B). CAO was performed at time point "0 s". MABP was significantly higher in NOS3 KO animals at all time points (A), whereas ΔMABP differed from 210 s (B). Mean ± SEM, two-way ANOVA and Bonferroni's post hoc test. Note the enhanced time resolution between (A) or before (B) the dashed lines.

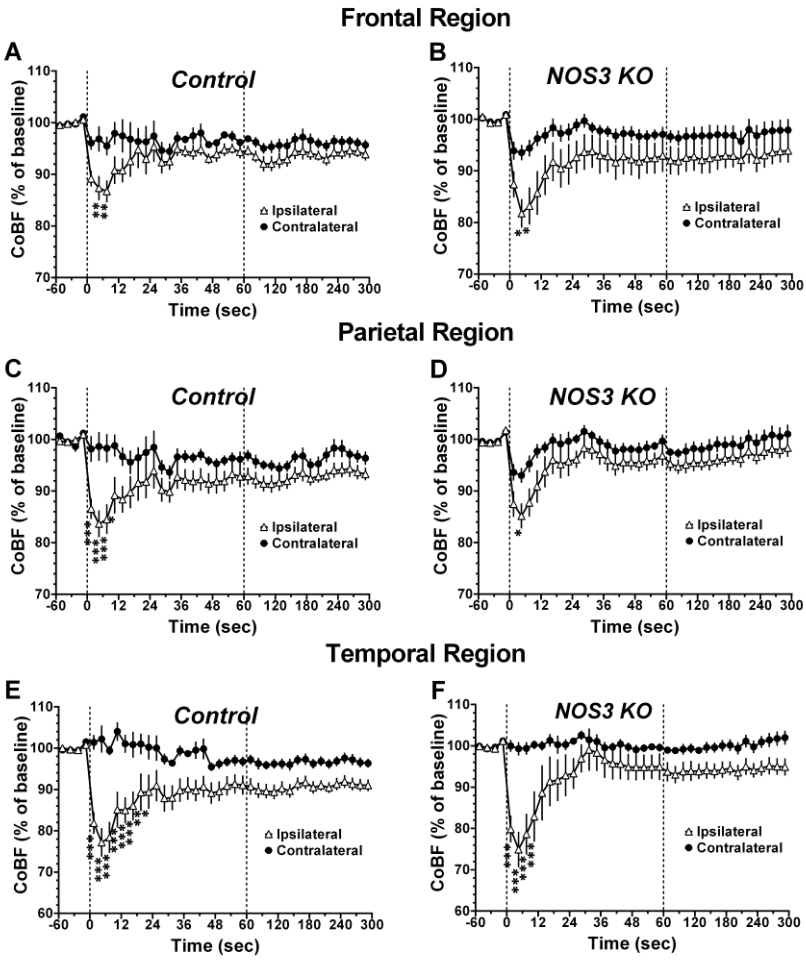

Fig. 2. Regional cerebrocortical blood flow (CoBF) in control (n = 12; A, C, and E) and NOS3 KO (n = 11; B, D, and F) mice before and after carotid artery occlusion (CAO). CoBF is expressed as a percentage of the baseline, i.e., the averaged values in 1 min preceding CAO. Open triangles and closed circles represent CoBF in the ipsilateral and contralateral hemispheres, respectively. Mean ± SEM, two-way ANOVA and Bonferroni's post hoc test. Note the enhanced time resolution between the dashed lines.

The reduction of CoBF in the acute phase was significantly higher in the temporal cortex of both the control and NOS3 KO animals compared to the frontal and parietal regions (Fig. 3A). In the ipsilateral frontal and parietal regions of NOS3 KO animals, similar maximal reductions could be obtained, with no significant differences compared to the controls (Fig. 3A). Furthermore, in the subacute phase, similar CoBF reductions have been detected in the frontal, parietal and temporal regions of control and NOS3 KO animals (Fig. 3B).

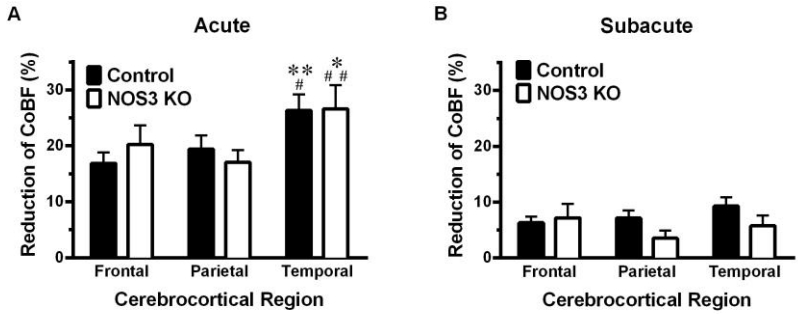

Fig. 3. Regional cerebrocortical blood flow (CoBF) reductions during the acute (A) and subacute (B) phases after CAO in the ipsilateral hemisphere of control (filled bars, n = 12) and NOS3 KO (open bars, n = 11) mice. CoBF values have been determined at their minimum ("Acute") or 5 min after CAO ("Subacute"), and reductions are expressed as a percentage of the baseline, i.e., the average CoBF in 1 min preceding CAO. Mean ± SEM, *$p<0.05$, **$p<0.01$ vs. "Frontal"; #$p<0.05$, ##$p<0.01$ vs. "Parietal" with two-way ANOVA and Bonferroni's post hoc test.

4.2 The effects of NOS1 deletion and general NO deficiency on the CoBF changes after CAO

4.2.1 Morphological parameters of leptomeningeal collaterals

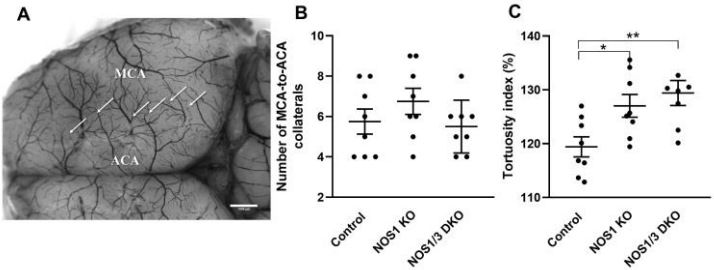

Fig. 4. Morphology of leptomeningeal collaterals in control, NOS1 KO, and NOS1/3 DKO mice. Panel (A) shows a representative image of the cerebrocortical vessels in a control mouse brain. The arrows indicate the leptomeningeal collaterals between the territories of the middle cerebral artery (MCA) and anterior cerebral artery (ACA). (B) Number of MCA-to-ACA collaterals. No significant difference in the number of collaterals was observed between the groups. (C) Tortuosity index. The tortuosity index is significantly increased in NOS1 KO and NOS1/3 DKO animals compared to controls. Scatter dot plots with mean ± SEM are shown, one-way ANOVA with Tukey's post hoc test.

4.2.2 Blood pressure of NOS1 KO, NOS1/3 DKO and L-NAME-treated mice

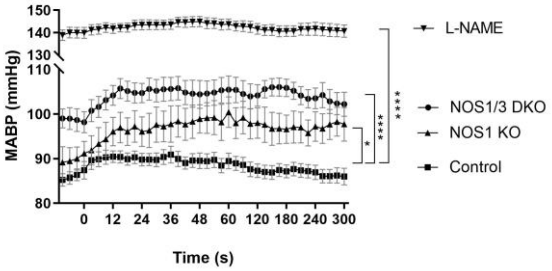

Fig. 5. Mean arterial blood pressure in control, NOS1 KO, NOS1/3 DKO, and L-NAME treated control mice. The zero point on the x-axis represents the time of carotid artery occlusion. NO deficiency resulted in elevated blood pressure in the NOS1 KO, NOS1/3 DKO, and L-NAME treated mice compared to the control group. Mean ± SEM, two-way ANOVA. The number of animals (n) was 10, 6, 11, and 15 in the control, NOS1 KO, NOS1/3 DKO, and L-NAME groups, respectively.

4.2.4 Changes in regional CoBF following unilateral CAO

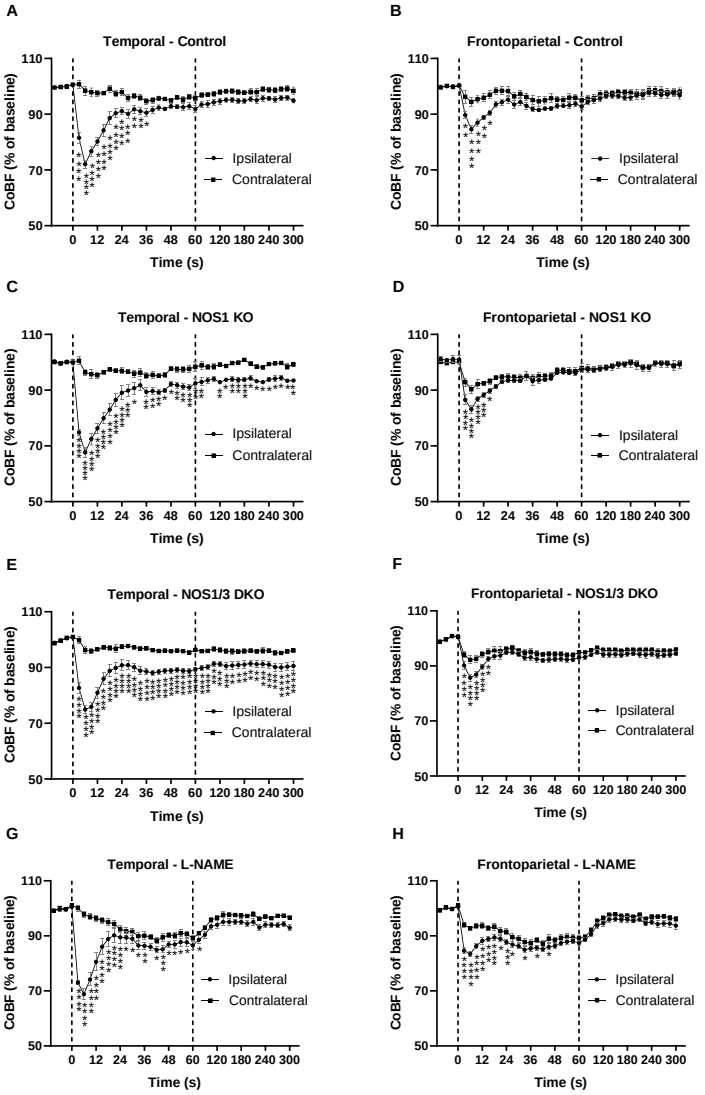

Fig. 6. Cerebrocortical blood flow (CoBF) in the ipsilateral and contralateral hemispheres after unilateral carotid artery occlusion (CAO). Panels A and B: CoBF in temporal (A) and frontoparietal (B) regions in control mice (n=10) after unilateral CAO. In both ipsilateral regions, the blood flow normalizes after a transient reduction post-CAO. Panels C and D: CoBF in temporal (C) and frontoparietal (D) regions in NOS1 KO animals (n=6) after unilateral CAO. Note the less complete recovery in the temporal region compared to the frontoparietal region. Panels E and F: CoBF in temporal (E) and frontoparietal (F) regions in NOS1/3 DKO animals (n=11) after unilateral CAO. Note the sustained hypoperfusion in the temporal region but not in the frontoparietal region. Panels G and H: CoBF in temporal (G) and frontoparietal (H) regions of L-NAME treated animals (n=15) after unilateral CAO. Note the acute severe hypoperfusion in both regions of the ipsilateral hemisphere and mild hypoperfusion of the contralateral hemisphere in the first 90 seconds after CAO and the recovery of CoBF in both regions thereafter. Values are presented as mean ± SEM percentage of the baseline. Circles indicate the ipsilateral, whereas squares the contralateral hemisphere, two-way ANOVA with Bonferroni's post hoc test). Note the enhanced time resolution between the dashed lines.

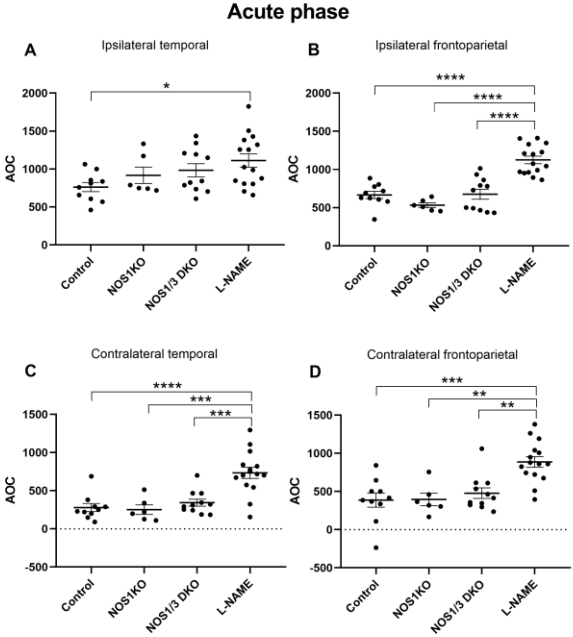

Fig. 7. Comparison of hypoperfusion levels determined by area over the curve (AOC) values of blood flow in control, NOS1 KO, NOS1/3 DKO, and L-NAME treated control mice (n=10, 6, 11, 15, respectively) in the acute phase (6-90 sec) after unilateral carotid artery occlusion. L-NAME treated animals significantly differ from controls in the ipsilateral temporal region (A) and from all other groups in the ipsilateral frontoparietal region (B). Furthermore, L-NAME treated animals significantly differ both in the contralateral temporal (C) and the frontoparietal regions (D) from all other groups. Scatter dot plots with mean ± SEM are shown. Statistical analysis was performed with one-way ANOVA and Tukey's post hoc test.

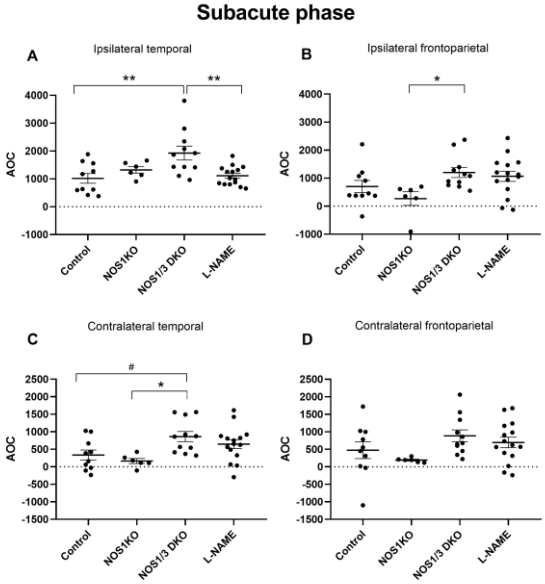

Fig. 8. Comparison of hypoperfusion levels determined by AOC (area over the curve) values of blood flow in control, NOS1 KO, NOS1/3 DKO, and L-NAME treated wild type mice (n=10, 6, 11, 15, respectively) in the subacute phase (90-300 sec) after unilateral carotid artery occlusion. NOS1/3 DKO animals show worsened recovery in the ipsilateral temporal (A) and frontoparietal (B) regions. The blood flow recovery of NOS1/3 DKO mice is also compromised in the temporal (C, #p=0.0514) but not in the frontoparietal region (D) of the contralateral hemisphere. Scatter dot plots with mean ± SEM are shown. Statistical analysis was performed with one-way ANOVA and Tukey's post hoc test.

5. Conclusions

- The existing macrovascular connections (i.e., the arteries of the Willis circle) are insufficient to compensate immediately and completely for the loss of one CCA, and active vasoregulation is required to adapt the cerebrocortical circulation to the altered hemodynamic situation.
- The temporal pattern of the CoBF recovery after CAO suggests the significance of an active cerebrovascular vasodilator mechanism driven by metabolic, endothelial, or neuronal signals.
- Intracortical redistribution of the CoBF, presumably via pial anastomoses between the MCA and AACA, appears to attenuate the ischemia of the most severely affected temporal cortex at the expense of reducing the blood perfusion of the frontoparietal regions.
- The lack of endothelial nitric oxide synthase (NOS3) alone does not impair the recovery after unilateral CAO.
- Mice lacking neuronal nitric oxide synthase (NOS1 KO) and double knockout mice of NOS1 and NOS3 (NOS1/3 DKO) exhibit impaired cerebrocortical blood flow adaptation to CAO, particularly in the subacute phase.
- Pharmacological inhibition of NO synthesis with L-NAME results in severe alterations in CBF, mainly in the acute phase.
- The unfavorable morphological development (increased tortuosity) of the leptomeningeal collaterals and lack of NO-mediated vasodilation may be responsible for the prolonged hypoperfusion of the brain in NOS1/3 DKO mice.

6. Bibliography of the candidate's publications

Publications related to the dissertation:

Polycarpou A, Hricisák L, Iring A, Safar D, Ruisanchez É, Horváth B, Sándor P, Benyó Z. Adaptation of the cerebrocortical circulation to carotid artery occlusion involves blood flow redistribution between cortical regions and is independent of eNOS. Am J Physiol Heart Circ Physiol. 2016;311(4):H972-h980. **IF: 3.348**

Hricisák L, Pál É, Nagy D, Delank M, Polycarpou A, Fülöp Á, Sándor P, Sótonyi P, Ungvári Z, Benyó Z. NO Deficiency Compromises Inter- and Intrahemispheric Blood Flow Adaptation to Unilateral Carotid Artery Occlusion. Int J Mol Sci. 2024;25(2). **IF: 5.563**

Publications not related to the dissertation:

Molnár E, Molnár B, Lohinai Z, Tóth Z, Benyó Z, Hricisák L, Windisch P, Vág J. Evaluation of Laser Speckle Contrast Imaging for the Assessment of Oral Mucosal Blood Flow following Periodontal Plastic Surgery: An Exploratory Study. Biomed Res Int. 2017;2017:4042902. **IF: 2.583**

Iring A, Hricisák L, Benyó Z. CB1 receptor-mediated respiratory depression by endocannabinoids. Respir Physiol Neurobiol. 2017;240:48-52. **IF: 1.792**

Pál É, Hricisák L, Lékai Á, Nagy D, Fülöp Á, Erben RG, Várbíró S, Sándor P, Benyó Z. Ablation of Vitamin D Signaling Compromises Cerebrovascular Adaptation to Carotid Artery Occlusion in Mice. Cells. 2020;9(6). **IF: 4.366**

Hinsenkamp A, Ézsiás B, Pál É, Hricisák L, Fülöp Á, Besztercei B, Somkuti J, Smeller L, Pinke B, Kardos D, Simon M, Lacza Z, Hornyák I. Crosslinked Hyaluronic Acid Gels with Blood-Derived Protein Components for Soft Tissue Regeneration. Tissue Eng Part A. 2021;27(11-12):806-820. **IF: 3.776**

Gölöncsér F, Baranyi M, Iring A, Hricisák L, Otrokocsi L, Benyó Z, Sperlágh B. Involvement of P2Y(12) receptors in a nitroglycerin-induced model of migraine in male mice. Br J Pharmacol. 2021;178(23):4626-4645. **IF: 9.473**

Császár E, Lénárt N, Cserép C, Környei Z, Fekete R, Pósfai B, Balázsfi D, Hangya B, Schwarcz AD, Szabadits E, Szöllősi D, Szigeti K, Máthé D, West BL, Sviatkó K, Brás AR, Mariani JC, Kliewer A, Lenkei Z, Hricisák L, Benyó Z, Baranyi M, Sperlágh B, Menyhárt Á, Farkas E, Dénes Á. Microglia modulate blood flow, neurovascular coupling, and hypoperfusion via purinergic actions. J Exp Med. 2022;219(3). **IF: 15.319**

Csomó KB, Varga G, Belik AA, Hricisák L, Borbély Z, Gerber G. A Minimally Invasive, Fast Spinal Cord Lateral Hemisection Technique for Modeling Open Spinal Cord Injuries in Rats. J Vis Exp. 2022(181). **IF: 1.216**

Hinsenkamp A, Fülöp Á, Hricisák L, Pál É, Kun K, Majer A, Varga V, Lacza Z, Hornyák I. Application of Injectable, Crosslinked, Fibrin-Containing Hyaluronic Acid Scaffolds for In Vivo Remodeling. J Funct Biomater. 2022;13(3). **IF: 4.842**

Őrfi E, Hricisák L, Dézsi L, Hamar P, Benyó Z, Szebeni J, Szénási G. The Hypertensive Effect of Amphotericin B-Containing Liposomes (Abelcet) in Mice: Dissecting the Roles of C3a and C5a Anaphylatoxins, Macrophages and Thromboxane. Biomedicines. 2022;10(7).
IF: 4.669

Nagy D, Hricisák L, Walford GP, Lékai Á, Karácsony G, Várbíró S, Ungvári Z, Benyó Z, Pál É. Disruption of Vitamin D Signaling Impairs Adaptation of Cerebrocortical Microcirculation to Carotid Artery Occlusion in Hyperandrogenic Female Mice. Nutrients. 2023;15(18).
IF: 5.863

Iring A, Baranyi M, Iring-Varga B, Mut-Arbona P, Gál ZT, Nagy D, Hricisák L, Varga J, Benyó Z, Sperlágh B. Blood oxygen regulation via P2Y12R expressed in the carotid body. Respir Res. 2024;25(1):61. **IF: 4.058**

∑IF: 71.176